15

Optimization of technologies for manufacturing integrated photonics structures using positive electron resist AR-P 6200

© V.A. Kiselevskiy[1,2], K.A. Fetisenkova[2,3], A.A. Tatarintsev[2], A.E. Melnikov[2], O.G. Glaz[2]

[1] Institute of Ultra High Frequency Semiconductor Electronics of RAS, Moscow, Russia
[2] Valiev Institute of Physics and Technology, Russian Academy of Sciences, Moscow, Russia
[3] Moscow Institute of Physics and Technology (State University), Dolgoprudny, Russia

E-mail: sevakiselevskiy@yandex.ru

Received October 29, 2024
Revised December 17, 2024
Accepted February 28, 2025

A method for manufacturing waveguides with a channel of a given width using electron-beam lithography with the application of positive electron resist AR-P 6200 (CSAR 62) was developed. A technological process with selected parameters was found, which made it possible to manufacture test structures of integrated photonics.

Keywords: fiber optics, electron beam lithography, reactive-ion etching, positive electron resist.

DOI: 10.61011/EOS.2025.03.61163.2-25

Introduction

An intensive development of integrated photonics has been recently observed. Technological maturity, as well as compact size and convenience of configuration of photonics elements on silicon substrates has a huge advantage for the implementation of photonic structures using modern semiconductor production methods. Projection photolithography systems are mainly used for the production of photonic integrated circuits since the productivity of electron lithography equipment is insufficient for mass production. Steppers are often used together with electron-beam lithography (EBL) to create input and output gratings. Such projects are implemented, for example, by Optoelectronics Research Centre, CUMEC and other organizations. However, the use of photolithography for mask formation is not always justified because of the complexity and cost of production of photographic templates, as well as the roughness requirements for the waveguide edge [1]. EBL is an alternative way for creating the topology of photonic structures for research activities as well as for small-scale production [2,3].

Silicon has recently attracted much attention as a material for highly integrated photonics. It has low loss for the optical coupling window (1.8−2.0 dB/cm), a refractive index of 3.5 at telecommunication wavelengths, and it allows producing low-cost optoelectronic solutions for applications of various scales — from long distances to chip-to-chip links. Moreover, silicon photonic devices can be fabricated using standard silicon processing technology. Compatibility with complementary metal-oxide-semiconductors (CMOS) allows for relatively low-cost production of monolithically integrated optoelectronic structures. It is possible to achieve channels sizes with height and width of up to $0.2 \times 0.5\,\mu$m, respectively in the production of waveguides based on silicon-on-insulator structures [4].

There is a relationship between the geometric parameters of the waveguide and the wavelength of the transmitted radiation [1,5]. The wavelength of the propagating radiation should be comparable to the transverse dimension of the waveguide for the propagation of a wave with acceptable losses. The emission with wavelengths of the visible spectrum as well as near-infrared radiation is used in the integrated optics applications. Waveguides with a cross-section size smaller than the wavelength of the propagating radiation are also used in integrated optical devices. For example, such nanowires having a length of less than $200\,\mu$m are used for connecting a waveguide to a resonator [6].

When producing photonic structures, their geometrical parameters are determined both by the addressed task and by the resolution and capabilities of the technological processes and materials used [7]. Nonconformities of the dimensions of fabricated waveguide structures and the dimensions calculated during designing can result in serious errors in waveguide operation in various integrated optical devices. For example, any change of the waveguide width by 1 nm results in a wavelength error of about 1 nm in the transmission spectra of Mach-Zehnder interferometers, microresonators, or photonic crystal resonators [8].

EBL technology is commonly used for prototyping and fabrication of fiber and photonic optics structures. EBL is a highly accurate and technologically advanced method because of its high resolution in forming structures. EBL technology allows relatively fast and cheap prototyping of structures for further research or use.

The resolution of the EBL is determined by the size of the electron probe, electron beam energy, properties of electron resists, and development parameters. Although EBL technology has been improved over the years, there is still a need to optimize both the technology itself and the process parameters taking into account the characteristics of the electron-beam resist (sensitivity, resolution, and

contrast) to enhance performance. The plasma resistance of the resist mask is an equally important parameter for forming waveguide structures using an electron resist mask. This characteristic is crucial for creating structures with high aspect ratio [9]. The use of an electron resist mask for the plasma chemical etching (PCE) process allows avoiding additional process operations to remove the rigid mask as well as contamination of materials with relevant impurities. In most cases, the polymer resistive mask can be easily removed in oxygen plasma.

Waveguides can be formed using both positive and negative electron resists. Such resists as HSQ [10–12] or AR-N 7520 [13] stand out among negative electron-beam resists due to their high resolution and plasma resistance. These resists are actively used for the formation of photonic structures by the EBL method. Fabrication of extended waveguides using a negative electron-beam resist requires high-precision alignment of the lithography system's writing fields to prevent discontinuities in the waveguide channel. The issue is that an electron-beam lithography (EBL) system can only pattern a field of up to a few hundred micrometers in length on the sample surface at a time. After this, the sample requires repositioning relative to the electron column to keep the patterned area within the column's focus. Writing field alignment errors can occur when the table with the sample is displaced, resulting in waveguide channel discontinuity. Channel discontinuities will significantly affect the signal intensity loss as it travels along the waveguide. However, it is impossible to increase the writing field dimensions sufficiently to fit the entire structure within a single patterned area, because the increase of the writing field size reduces fabrication accuracy and increases edge roughness of the structures. Also, as a general rule, a negative resist requires a higher dosage. Thus, the use of negative resists is not always appropriate because of complicated handling and the stability requirements of the EBL setup, especially for large-scale structures.

Lithography using a positive electron resist such as AR-P 6200 can become an alternative [14]. A pattern is formed in this method around the silicon waveguide in positive resist for further etching. The inevitable alignment errors will not cause any interruption of the waveguide channel, since in this case it is not the waveguide itself that is treated, but the area around it. Defects resulting from alignment errors can be partially or completely removed by subsequent PCE because they have small linear dimensions and are outside the waveguide. Also, the writing field (~ 20 nm) was slightly enlarged as part of the lithography parameter refinement to avoid discontinuities along the waveguide channel on the lithography setup used. A waveguide structure surrounded by an etched volume is obtained after the PCE process. In the next step, the etched volume can be filled with silicon oxide and the wafer can undergo a planarization procedure.

Positive electron resist AR-P 6200 or CSAR 62 (Allresist) belongs to the group of styrene acrylates. Poly(α-methylstyrene-co-methylchloracrylate), acid generator and anisole solvent are the main components of the resist. The polymer layers are furthermore thermally stable up to 240 °C, with a glass transition temperature of 148 °C. CSAR 62 has better sensitivity and plasma resistance compared with polymethyl methacrylate (PMMA) based resists. The high sensitivity of the resist is achieved by introducing halogen atoms into the polymer chain [9,14]. Chlorine is usually used for this purpose (as for CSAR 62 — methyl chloracrylate), but bromine or iodine are also used [14]. Chlorine atoms support polymer chain breakage in case of the electron irradiation, and the halogen-containing acid generator enhances this effect [14]. As a result, less energy (lower exposure dose) is required to separate the high molecular weight polymer into smaller fragments. These fragments rapidly dissolve in the developer, while the non-exposed, still high molecular weight regions of the resist are not exposed to the developer. The addition of a thermostable acid generator gave this resist its name, chemical amplified resist (CSAR). Since the acid generator is activated during the electron irradiation process, the layers do not require an annealing process after exposure [15].

Good plasma resistance is achieved by introducing aromatic substituents such as, for example, phenyl, naphthyl or anthracyl groups into the polymer [14]. In addition, CSAR contains α-methylstyrene for ensuring etch resistance. Due to their π-electrons, the aromatics are much more stable in the presence of various plasmas compared to aliphatic polymers such as PMMA, and thus achieve a high level of stability close to photoresists. Photoresists primarily consist of novolacs (mixtures of cresols condensed with formaldehyde) which, due to their cresol content, exhibit high aromatic density and consequently demonstrate greater stability in plasma etching processes [14,15].

Thus, the resist AR-P 6200 CSAR 62 has the necessary characteristics suitable for prototyping and small-scale production of fiber structures. An additional advantage is the convenience of subsequent planarization of integrated optics devices made with positive resist, should this become necessary.

The dimensions of fiber optics structures obtained by the EBL method should correspond to the dimensions obtained by modeling and calculations with the minimum possible deviation, since the change in the dimensions of optical structures has a very strong influence on the number of modes and correctness of the device operation in the future. The results presented in this paper will make it possible to select the process parameters such as the dosage and size of the template structures to obtain the final structures with the required characteristics with an error of less than 10 nm.

Experimental methodology

Silicon-on-insulator (SOI) wafers were used to test the resists. 220 nm silicon layer on 2 μm thick silicon oxide was applied to a silicon wafer with orientation (100). The SOI wafers were cleaned in oxygen plasma for 2 min with a

gas flow of 50 sccm before resist application. AR-P 6200 (CSAR 62) resist with a concentration of 4 % (anisole diluent) was applied to the prepared wafers using SM-180 centrifuge (SAWATEC AG, Switzerland) at a target speed of 4000 rpm. The centrifuge table was rotated at a speed of 300 rpm at the initial stage with an angular acceleration of 300 rad/s^2 to evenly distribute the resist on the wafer surface. The rotation of the centrifuge table at 300 rpm was maintained for 5 s. Then, the table reached the target rpm within a time of 5 s and this speed was maintained for 60 s. The resist was dried after application using hotplate HP-200 (SAWATEC AG, Switzerland) at 150 °C for 240 s in a nitrogen atmosphere.

The spectral ellipsometry method was used to control the thickness of the deposited layers, providing an error of 1 nm or less and an acceptable spatial resolution over the wafer area. Measurements were performed using spectral ellipsometer M-2000X (J.A. Woollam Co., Inc., USA) in a set up with a constant beam angle (65°) in the wavelength range of 246.3–999.8 nm.

Wafer exposure was performed using the Raith-150 system (Raith, Inc., Germany) at a maximum beam energy of 30 keV with a 30 μm aperture, producing an electron beam of approximately 1 nm in diameter and up to 120 pA current. Immediately prior to exposure, the probe current was measured using a Faraday cylinder, after which the beam dwell time at each exposure point was recalculated. Exposure of the lines with the smallest size was performed at the maximum electron energy $E_0 = 30$ keV. The template for exposing the test structures consisted of a set of lines of different widths. Such a template consisted of lines with widths ranging from 500 to 850 nm in 50 nm increments for obtaining 500 nm lines. The template consisted of lines with widths ranging from 4500 to 4710 nm in 70 nm increments for obtaining 4500 nm lines. Silicon waveguides with channel widths from 500 nm to 10 μm and lengths from 5 to 20 mm were obtained. Exposure doses varied from 70 to 100 μC/cm^2 in increments of 10 μC/cm^2.

A series of tests were also carried out to obtain the lattice structure. The lattice structures were exposed to the electron beam energy of 30 keV with an aperture of 10 μm; the probe current at these parameters is 19 pA. The lattice structures were exposed with 4 nm increments in a 50 nm field. The exposure dose was constant at 100 μC/cm^2.

The wafers were etched in amyl acetate at room temperature (22 °C) for 60 s. The wafers were then treated in UHP isopropyl alcohol (IPA) for 30 s and dried by a stream of dry pure nitrogen. The wafers were not heated on a hotplate after the development.

Plasma chemical etching was performed using Dual PlasmaLab 100 (Oxford Instruments Plasma Technology, UK) with inductively coupled plasma (ICP) of SF6/C4F8 gases excited at 2 MHz. The controlled bias on the sample was generated by a high-frequency oscillator with a frequency of 13.56 MHz, which produced an equivalent DC bias voltage VDC in the range of 80 – 150 V. Wafers were segmented to obtain a set of samples with identical

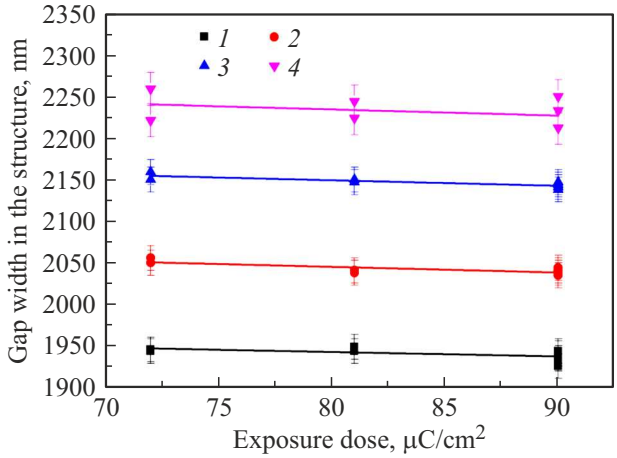

Figure 1. Dependence of the line gap width on the line exposure dose after the etching process. With the width of the gap in the template: *1* — 2000 nm ($y = 1985.27273 - 0.5303 \times$ Dose), *2* — 2100 nm ($y = 2099.63636 - 0.68182 \times$ Dose), *3* — 2200 nm ($y = 2202.5 - 0.66667 \times$ Dose), *4* — 2300 nm ($y = 2293.68182 - 0.74242 \times$ Dose).

line groups. The base pressure in the reactor chamber was 10 – 6 Torr. Plasma chemical etching of the samples was performed with a SF6 fraction in the plasma mixture equal to 22 % and a bias voltage equal to 100 V. The time of the etching processes was the same for all images and amounted to 100 s. The etching depth was 200 nm.

Images of the structure profiles after the etching process, as well as structure parameters, were obtained using scanning electron microscope Ultra 55 (SEM) (Carl Zeiss AG, Germany) with a spatial resolution of $\sim$ 1 nm.

Results and discussion

The areas near the waveguide channel are exposed in the waveguide lithography using positive electron resist. While exposure doses of 80 – 100,μC/cm^2 achieve full resist development, they induce lateral feature size variations in the exposed regions, resulting in reduced waveguide channel dimensions. Reducing the dose does not result in the full development of the resist and makes the situation much worse. Thus, it was found that during the positive electron resist process, the actual channel width of the waveguide differs from the channel width specified in the lithographic template. This reduction of the waveguide channel is associated with the overexposure of neighboring regions (proximity effect), the sensitivity and contrast of the selected resist, and the development parameters (in particular, the developer temperature). The size of the structures obtained after development is determined by parameters such as the selected exposure dose and external factors affecting the reduction in the size of the structures during the development process. It is possible to correct the effect of reducing the size of the formed structures by optimal

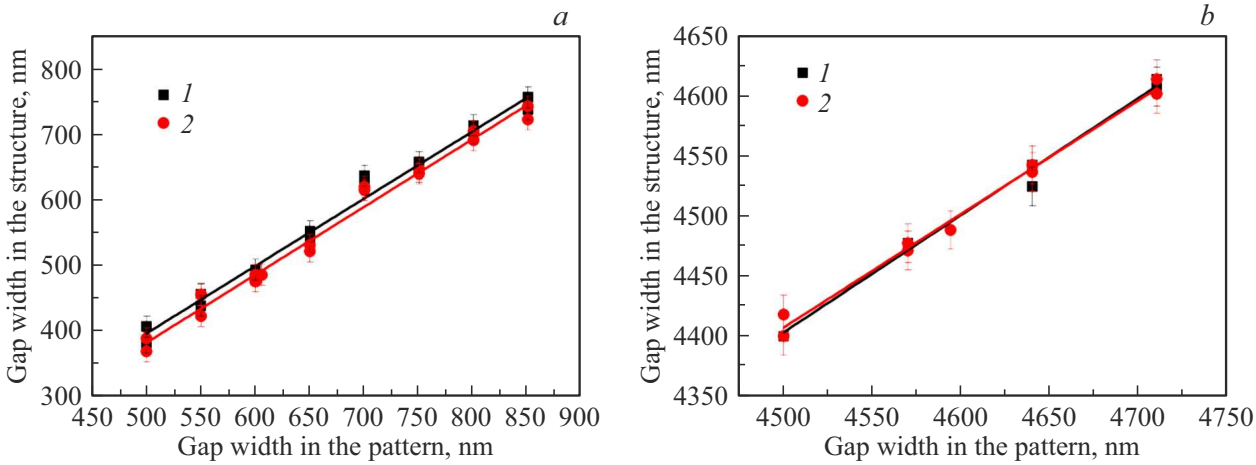

Figure 2. Dependence of the gap width of the final structure on the gap width of the original template. (*a*) Template width 500 nm: (*1*) $y = -120.05357 + 1.03369x$, (*2*) $y = -138.11862 + 1.04147x$. (*b*) Template width 4500 nm: (*1*) $y = 24.38462 + 0.97308x$, (*2*) $y = 162.83018 + 0.9432x$. Data are presented for lines obtained at doses of 90 (*1*), 100 μC/cm^2 (*2*) after etching for 100 s.

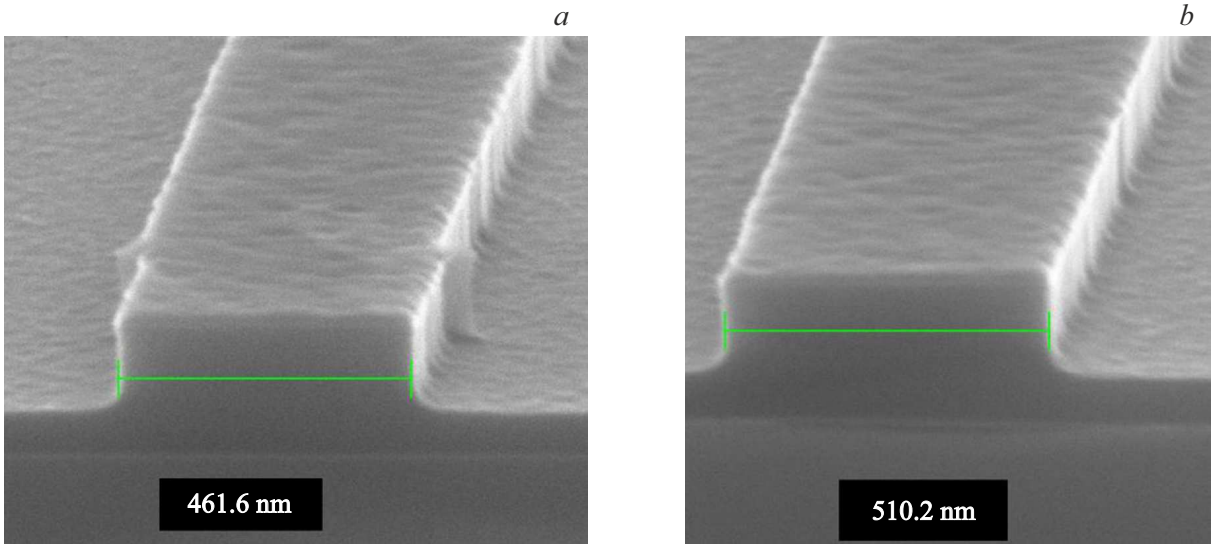

Figure 3. Images of chips of channels of silicon structures after etching at lithographic template gap widths of 560 (*a*), 570 nm (*b*).

selection of the dose, as well as correction of the width of the exposed areas.

Insoluble resist fragments sometimes remain on the surface of the exposed region in case of lithography AR-P 6200 with $80 - 95\,\mu$C/cm^2 dose. Anisotropic cleaning of the resist in oxygen plasma at a pressure of 10 mTorr and an oxygen flux of 10 sccm and a power of 40 W in a RF reactor for 30 s was used to remove these fragments prior to etching. Since the main interest is the actual width of structures in silicon after the etching process, here we present the results after PCE of silicon in a mixture of gases C_4F_6 and SF_6 with fluxes of 48 and 22 sccm, respectively, at a pressure of 10 mTorr. The power supplied to the RF reactor was 10 W, the power supplied to the ICP reactor was 1200 W. The etching time was selected based on the desired etching depth. All dimensions in the presented graphs are given based on the results of measurement of silicon etched through the silicon resistive mask.

Selection of the dose for exposed sections of the linear part of the waveguides

A series of tests were performed with line exposure doses of 70, 80, 90 μC/cm^2 to study the effect of exposure dose on line width at fixed line sizes in the template (Fig. 1). It should be noted that the line width variation with dose change is minimal, ensuring a stable process window for dose.

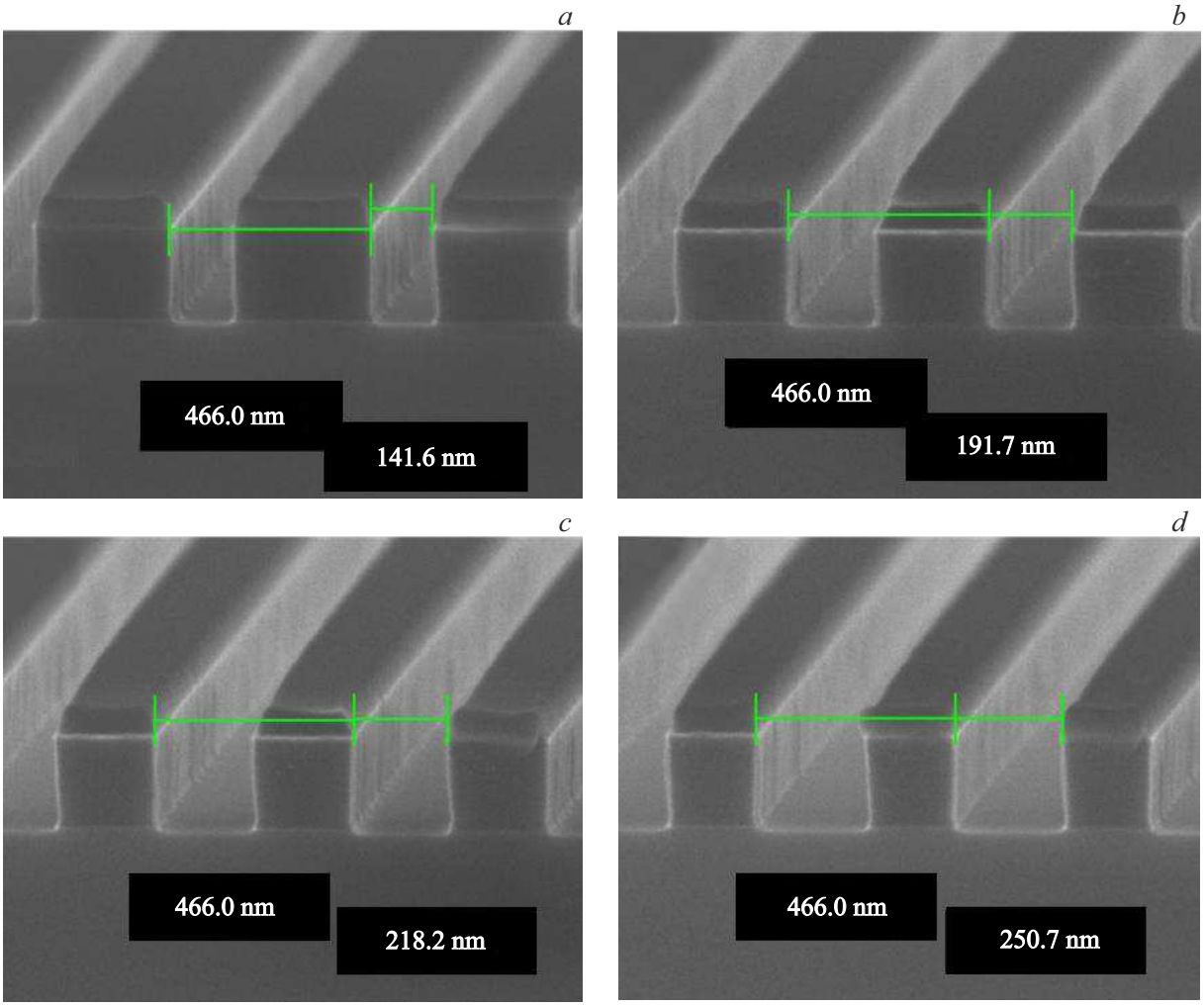

Figure 4. The width and period of lines of different thicknesses exposed and etched to a depth of 200 nm with a period of 465 nm: template line width 100 (a), 150 (b), 175 (c), 200 nm (d).

As can be seen from the figure, the final line width insignificantly changes in the range of the mentioned doses. Consequently, this parameter can be fixed and can be disregarded when selecting the line width.

Selection of the width of the exposed linear part of the waveguide

It is possible to correct the change of the size of structures that occurs because of external factors in the process of development and exposure by selecting the size of the template for exposure. Structures with channel widths on the order of 500 nm are quite common in the modern fiber optics when high dimensional accuracy is required.

Channel width measurements in silicon structures after PCE have been performed in the study. The structures were exposed using templates with different gap widths ranging from 500 to 850 nm in 50 nm increments (Fig. 2, a), and templates with widths ranging from 4500 to 4710 nm in 70 nm increments (Fig. 2, b).

SEM images of examples of structures obtained for different gap widths in the template during measurements performed for 500 nm channels are shown in Fig. 3.

Fig. 2 shows that the width of the obtained structures varies linearly with the lithographic template width. Similar procedures for selecting the gap width in the lithographic template have been successfully carried out for waveguides with channel widths of 2.5 and 6.5 μm. The values of the gap width between the two lithography regions that provide the required waveguide channel width were found in these experiments.

Selection of exposure parameters to produce periodic structures In addition to the fiber channel, fiber and integrated optics devices may include periodic structures for input and output of radiation into the waveguide channel such as diffraction gratings. When fabricating such structures, the conformity between designed and actual

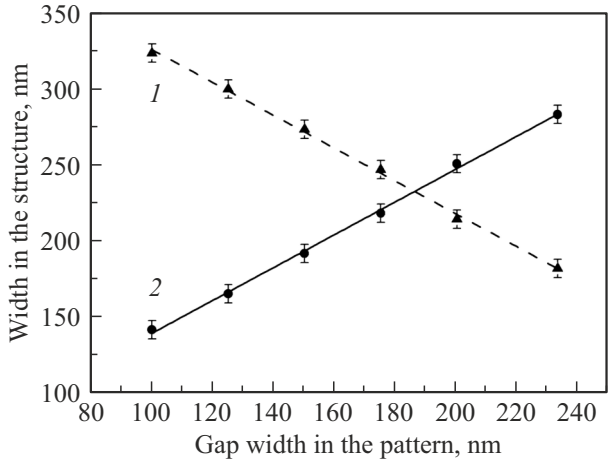

Figure 5. The dependence of the line width after etching on the line width in the template. LSM approximation. Lines of different widths with period of 465 nm: (*1*) line width dependence, (*2*) line gap width dependence.

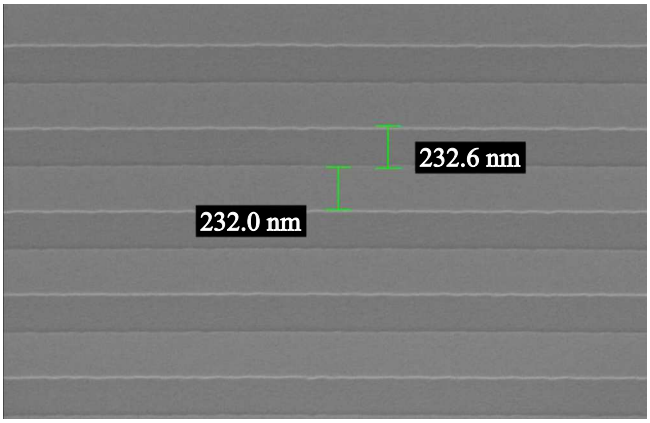

Figure 6. Example of a formed waveguide grating.

dimensions is equally as critical as for waveguide channel formation. This section describes the methodology for optimizing lithography parameters to fabricate diffraction gratings with predefined periods on silicon wafers.

The necessary template width was selected for obtaining gratings with a period of 465 nm and a filling factor of 0.5. The lithography dose in this case was 100 6μC/cm^2. Fig. 4 shows SEM images of the profiles of the obtained structures after the etching process.

The dependence of the line width after etching on the line width in the template was obtained (Fig. 5). The dependence was approximated by the least square method (LSM).

A line width of 233 nm with a lattice constant of 465 nm is obtained with an actual pattern line width of 186 nm according to the calculation. The lattice lines in the template were changed to 186 nm in subsequent lithographies. The etching depth was selected based on the etching time and can be varied as needed.

Fig. 6 shows the SEM image of the lattice structure obtained at a line width of 186 nm in the template.

Thus, the adjustment of the line size in the template according to the calculations allows obtaining a lattice structure with a line width of 232 nm and a lattice period of 465 nm.

Conclusion

The parameters for lithography of fiber and periodic structures applicable to integrated optics were selected in this study, taking into account the process features of the selected resist AR-P 6200 (CSAR). The dependences of the final line width on the dose were obtained, and it was concluded that it is possible to obtain the required width using any dose in the range of 70-100 μC/cm^2. The dependences of the final channel width on the lithographic template width are obtained, and approximating coefficients are found. It can be concluded that the final channel width differs from the lithographic template width by about 100 nm to the lesser side.

Using a well-established manufacturing process, test samples containing fiber structures with channel widths of 0.5, 2.5, 4.5, and 6.5 μm, as well as a test sample with a diffraction grating with a period of 465 nm, were fabricated. This technological process can also be applied to the fabrication of integrated optics structures with other dimensions of the same order with an error of less than 10 nm.

The study was performed under the state assignment to the Valiev Institute of Physics and Technology of RAS of the Ministry of Education and Science of the Russian Federation on the topic № FFNN-2022-0021.

Conflict of interest

The authors declare that they have no conflict of interest.

References

[1] D. Melati, A. Melloni, F. Morichetti. Adv. Opt. Photon., **6**, 156–224 (2014). DOI: 10.1364/AOP.6.000156
[2] R. Menon, A. Patel, D. Gil, H.I. Smith. Materials Today, **8** (2), 26–33 (2005). DOI: 10.1016/S1369-7021(05)00699-1
[3] U.D. Zeitner, M. Oliva, F. Fuchs, D. Michaelis, T. Benkenstein, T. Harzendorf, E-B. Kley, Appl. Phys. A, **109**, 789–796 (2012). DOI: 10.1007/s00339-012-7346-z
[4] L. Thylén, L. Wosinski. Photonics Research, **2** (2), 75–81 (2014). DOI: 10.1364/PRJ.2.000075
[5] K. Iizuka. *Engineering optics* (Springer, NY., 2008). Ch. 35, p. 316–317.
[6] A.H. Atabaki, S. Moazeni, F. Pavanello, H. Gevorgyan, J. Notaros, L. Alloatti, M.T. Wade, C. Sun, S.A. Kruger, H. Meng, K. Al Qubaisi, I. Wang, B. Zhang, A. Khilo, C.V. Baiocco, M.A. Popović, V.M. Stojanović, R.J. Ram. Nature, **556**, 349–354 (2018). DOI: 10.1038/s41586-018-0028-z

[7] Y. Su, Y. Zhang, C. Qiu, X. Guo, L. Sun. Adv. Mater. Technol., **5** (8), 1901153 (2020). doi.org/10.1002/admt.201901153
[8] P. Dong, W. Qian, H. Liang, R. Shafiiha, D. Feng, G. Li, J.E. Cunningham, A.V. Krishnamoorthy, M. Asghari. Opt. Express, **18**, 20298 (2010). DOI: 10.1364/OE.18.020298
[9] S. Thoms, D.S. Macintyre. J. Vacuum Sci. Technol. B, **32**, 6 (2014). DOI: 10.1116/1.4899239
[10] A.V. Myakonkikh, A.V. Shishlyannikov, A.A. Tatarintsev, V.O. Kuzmenko, K.V. Rudenko, E.S. Gornev. Mikroelektronika, **50** (5), 333–338 (2021) (in Russian). DOI: 10.31857/s0544126921050045
[11] A.A. Tatarintsev, A.V. Shishlyannikov, K.V. Rudenko, A.E. Rogozhin, A.E. Ieshkin. Mikroelektronika, **49** (3), 163?169 (2020) (in Russian). DOI: 10.31857/s0544126920030060
[12] A.V. Miakonkikh, N.A. Orlikovskiy, A.E. Rogozhin, A.A. Tatarintsev, K.V. Rudenko. Russ. Microelectron., **47** (3), 157–164 (2018). DOI: 10.1134/S1063739718030101
[13] K. Fetisenkova, A. Melnikov, V. Kuzmenko, A. Miakonkikh, A. Rogozhin, A. Tatarintsev, O. Glaz, V. Kiselevsky. Processes, **12** (9), 1941 (2024) (in Russian). DOI: 10.3390/pr12091941
[14] Allresist Positive E-Beam Resists AR-P 6200 (CSAR 62) product information [Electronic source]. URL: https://www.allresist.com/portfolio-item/e-beam-resist-ar-p-6200-series-csar-62/
[15] I. Kostic, K. Vutova, E. Koleva, R. Andok, A. Bencurova, A. Konecnikova. *Polymer science: research advances, practical applications and educational aspects* (2016). P. 488–497.

Translated by A.Akhtyamov